J Forensic Sci, Jan. 2005, Vol. 50, No. 1
Paper ID JFS2003224
Available online at: www.astm.org

Lee Hulse-Smith,[1] M.S.; Navid Z. Mehdizadeh,[2] Ph.D.; and Sanjeev Chandra,[2] Ph.D.

Deducing Drop Size and Impact Velocity from Circular Bloodstains

ABSTRACT: An experimental study was done to determine the diameter and velocity of blood drops falling on a surface by measuring the size of bloodstains they produced and counting the number of radial spines projecting from them. Bloodstains were formed by releasing drops of pig blood with a range of diameters (3.0–4.3 mm) and impact velocities (2.4–4.9 m/s), onto four different flat surfaces (glass, steel, plastic, paper) with varying roughness (0.03–2.9 μm). High-speed photography was used to record drop impact dynamics. Bloodstain diameters and the number of spines formed around the rim of stains increased with impact velocity and drop diameter. Increasing surface roughness reduced stain diameter and promoted merging of spines, diminishing their number. Equations are presented that explicitly relate drop diameter and impact velocity to measurements of stain diameter and number of spines.

KEYWORDS: forensic science, bloodstain pattern analysis, blood drop, pig blood, drop splashing

When investigators reconstruct details of a violent crime from physical evidence at the scene, it helps them to know the velocity with which blood drops spattered on surfaces. It has proved difficult, though, to accurately infer drop velocity by examining bloodstains. Attempts to correlate bloodstain diameter with impact velocity have not been very successful, since the size of a stain depends not only on the velocity but also the volume of blood that produced it. Different combinations of blood drop size and speed may result in almost identical stains.

Figure 1 illustrates the ambiguity inherent in deducing velocities from bloodstain size. It shows photographs of four stains, labeled *a-d*, produced by drops of pig blood falling onto a sheet of paper. The first bloodstain (Fig. 1*a*) was generated by a 3.7 mm diameter drop released from a height of 30.5 cm and the second (Fig. 1*b*) by a 3.0 mm diameter drop falling 121.9 cm. The stains have almost identical diameters, though impact velocities differed significantly. Similarly Figs. 1*c* and *d* show equal sized stains produced by drops with very different velocities. With two unknowns (drop velocity and size) and only one measurement (stain diameter), the problem appears insoluble. MacDonell (1) avoided this impasse by assuming a typical blood drop volume of 0.05 mL, corresponding to a diameter of 4.6 mm, when determining drop velocities from stain diameters. Pizzola et al. (2) questioned the validity of such an approach and demonstrated, using photographs similar to those in Fig. 1, the error created by variations in drop size. Given such uncertainties, bloodstains are currently classified on the basis of stain diameter as being "mist" (<0.1 mm), "fine" (0.1–2 mm), "medium" (2–6 mm) or "large" (>6 mm), without reference to velocity (3).

But bloodstains hold more information than just their size. Careful examination shows that while the stains in Figs. 1*a* and *b* have the same diameter, they are not identical. The periphery of each stain is wavy, with a number of regularly spaced spines, also referred to as rays, scallops, fingers or radial arms in the literature (1). The drop with the higher impact velocity (Fig. 1*b*) clearly has a greater number of spines; comparison of Figs. 1*c* and *d* confirms this trend. In a pioneering study Balthazard et al. (4) attempted to correlate the number of spines around stains with the height from which blood drops fell, but found that more spines could be produced by increasing either impact velocity or drop volume. They were unable to separate these two effects and concluded that using information about spines in forensic analysis required a better understanding of the fluid mechanics governing drop impact.

A number of models of drop impact dynamics have been developed in recent years for use in a variety of fields other than forensics, such as firefighting, spray cooling, ink-jet printing, pesticide spraying, spray painting, and liquid fuel combustion. Several analytical models available in the fluid mechanics literature (5–9) correlate both stain diameter and number of spines with drop diameter, velocity and liquid properties such as density, viscosity and surface tension. By measuring the diameter of a bloodstain and counting spines around it we could, in principle, determine both the size and velocity of the drop that produced it.

Application of drop impact models to bloodstain analysis faces two difficulties. First, models generally assume the surface on which drops land to be smooth and non-porous. A variety of surfaces are typically encountered at a crime scene and it is unclear how much variations in surface texture may affect drop impact dynamics. Second, models assume that drop physical properties are constant, whereas blood is a non-Newtonian fluid whose viscosity varies with shear rate (9). Experiments are necessary to determine how much uncertainty these two factors introduce into drop velocity calculations.

The principal objective of this study was to develop a method of deducing drop velocity and diameter from bloodstains. To achieve that we:

1. Measured the size of bloodstains formed by releasing drops of pig's blood (drop diameters 3.0–4.3 mm, velocities 2.4–4.9 m/s) onto a variety of surfaces (steel, glass, plastic laminate and paper);
2. Counted the number of spines around each bloodstain;

[1] Princess Margaret Hospital, 610 University Avenue, Toronto, Ontario, Canada M5G 2M9.
[2] Departmental of Mechanical & Industrial Engineering, University of Toronto, 5 King's College Road, Toronto, Ontario, Canada M5S 3G8.
Received 28 June 2003; and in revised form 21 Dec. 2003 and 2 Sept. 2004; accepted 2 Sept. 2004; published 8 Dec. 2004.

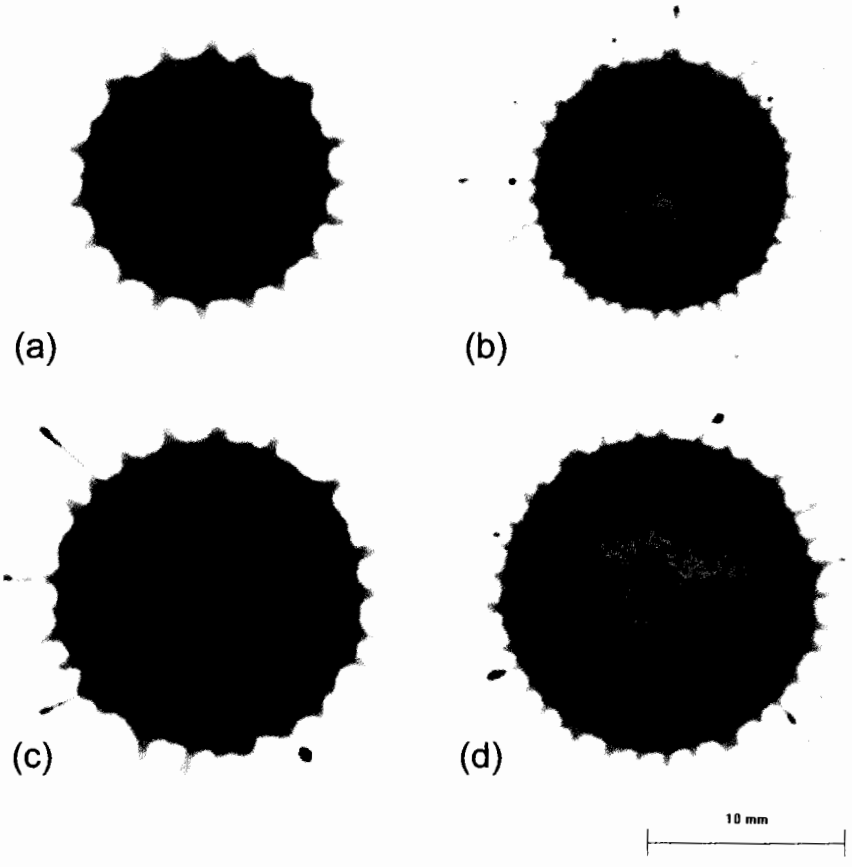

FIG. 1—*Two pairs of dried pig bloodstains with roughly equal diameters. Droplet diameter and release height were; a) 3.7 mm, 30.5 cm, b) 3.0 mm, 121.9 cm, c) 4.3 mm, 61.0 cm, d) 3.7 mm, 121.9 cm. The impact surface was paper.*

3. Confirmed the validity of using analytical models to predict stain diameter and number of spines;
4. Developed equations to predict drop velocity and size.

Materials and Methods

Alsever's pig blood (QueLab, Montreal, Quebec) was used for all experiments. The blood was kept at room temperature over a magnetic stirrer to prevent suspended blood cells from settling. Approximately 1 mL of blood was loaded into a 5 mL glass syringe clamped to a laboratory stand so that its height above a test surface resting on a flat lab bench could be varied. Blood drops were released by manually depressing the plunger of the syringe very slowly so that drops detached from the tip of a stainless steel hypodermic needle under their own weight. Three different flat-tipped needles were used to produce a range of drop sizes: needle dimensions and the average diameter of drops are listed in Table 1. The needle tip was cleaned after each release to prevent blood from drying along the needle circumference.

A FastCam-Ultima 1024 high-speed video camera (Photron, Tokyo, Japan) was used to photograph drop impact. The camera and Pallite VIII light source (Cooke, Auburn Hills, MI) was mounted above the impact surface. Light intensity was adjusted and a white cardboard reflector was placed around the surface to reflect light in an attempt to optimize image quality. A ruler was placed on the test surface and photographed before and after the experiment for image calibration and to ensure the camera had not accidentally been repositioned. Drops landing on the test surface were photographed at 2000 frames per second. Initial drop diameter (D_o) was measured 0.5 ms prior to impact using images from the high-speed camera. A total of 32 drops were measured for each needle using Image Pro Plus analysis software (Media Cybernetics, Silver Spring, MD). A single photograph was taken of the stain after all motion had ceased and the liquid began to dry. These images were used to measure stain diameter and number of spines.

TABLE 1—*Three drop diameters and standard deviation measured 0.5 ms prior to impact and the corresponding relevant needle dimensions. Drop diameter is used to calculate volume.*

Syringe Needle			
Inner Diameter (mm)	Outer Diameter (mm)	Droplet Diameter (mm), $n = 32$	Droplet Volume (μL)
0.55	0.8	3.0 ± 0.12	14
1.1	1.4	3.7 ± 0.05	27
2.2	2.7	4.3 ± 0.13	43

Four surfaces were tested: glass, stainless steel, 90 lb paper and a matte-white laminated surface typically installed on kitchen counters. Steel was the only surface requiring preparation, being polished on a metallurgical wheel with different grades of emery cloth to vary roughness. Each surface, with the obvious exception of paper, was washed with distilled water, dried with tissues and washed again with ethanol before reuse to ensure no residue was left on the surface. Surface roughness measurements were made for each surface using a PDI surfometer (Milan, MI) that records the profile of a surface by running a stylus over it. Table 2 lists the measured roughness of each surface, averaged over ten measurements made at different locations on each surface. Advanced contact angle was

TABLE 2—*Surface roughness and advancing contact angle measurements for the experimental test surfaces.*

Surfaces	Roughness (μm) $n = 10$	Advancing Contact Angle $n = 3$
Glass	0.03 ± 0.005	27 ± 1.2
Steel	0.89 ± 0.44	77 ± 3.8
Plastic	1.38 ± 0.11	70 ± 2.1
Paper	2.92 ± 0.21	...

TABLE 3—*Drop release height measured from the needle tip and converted to impact velocity using Eq 1.*

Release Height (cm)	Impact Velocity (m/s)
30.5	2.4
61.0	3.5
91.4	4.2
121.9	4.9

TABLE 4—*Published values for the physical properties of human blood, pig blood and distilled water.*

	Human Blood (12,13,14)	Pig Blood (12,13,14)	Distilled Water
RBC Volume (%)	40.0–45.0	38.9–46.3	...
Viscosity ($\times 10^{-3}$ kg/ms)	3.8–5.1	3.4–6.1	1.0
Surface Tension ($\times 10^{-2}$ N/m)	5.1–5.7	5.3–5.8	7.2
Density (kg/m^3)	1052–1063	1062	1000

also measured from profile photographs of drops moving across each surface, positioned at a 30° angle from the horizon.

Release height was measured from the needle tip to the test surface and converted to impact velocity (V_o) using the formula:

$$V_o = \sqrt{2gh} \quad (1)$$

where g is the acceleration due to gravity and h the release height. The effects of air resistance were neglected. Four different heights were used, which are listed in Table 3 along with the corresponding calculated impact velocities.

Blood consists of disc shaped red blood cells suspended in liquid plasma. It is a non-Newtonian fluid, meaning that its viscosity depends on flow rate. At low flow rates red blood cells aggregate, producing a large increase in viscosity. As flow increases shear stresses in the blood force cells to separate, reducing viscosity. At high enough shear rates (above 100 s^{-1}) the viscosity will eventually level off to a constant value (11). Blood drops experienced high enough shear rates during impact in this study that it was reasonable to assume that the physical properties of blood were constant. Values obtained from the literature (12–14) and used for calculations are listed in Table 4, along with physical properties of human blood and water. Properties of pig and human blood are very similar, and we expect drops of both to behave similarly. To confirm this we compared the size of pig bloodstains produced in our test with those of human blood measured by Willis et al. (15) whose experimental parameters were close to ours. They measured stains produced by dropping 4.2 mm diameter blood drops through distances of 30.5, 60.9, 91.4 and 121.9 cm, whereas in our experiments 4.3 mm drops were released from the same heights. In Fig. 2, data points represent the average diameter of 5 stains, with error bars marking the standard deviation. The results are seen to match closely with those of Willis et al. (15), confirming that pig blood drops behave very much like those of human blood.

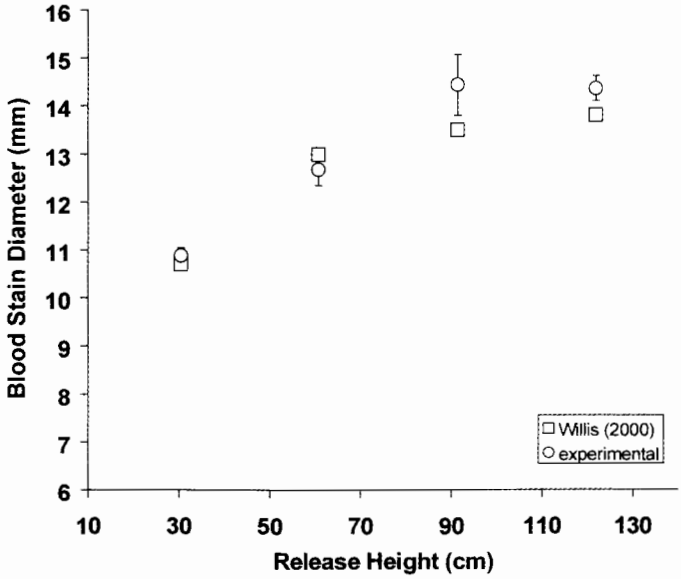

FIG. 2—*Experimental data for pig bloodstain diameter are compared with human bloodstain diameter results obtained by Willis (13). Droplet diameter was 4.3 mm and 4.2 mm for experiment and Willis respectively.*

Results and Discussion

Figure 3 shows photographs of three pig blood drops, each with different diameter (3.0 mm, 3.7 mm and 4.3 mm), landing on paper. The impact velocity in all cases was 4.2 m/s. Each column shows successive stages of drop impact, photographed from above with the camera pointing down at the sheet of paper. The time of each frame, measured from the moment of impact, is shown on the left of the pictures. The shadow of the falling drop on the surface was visible in the first row of pictures, making the drops appear slightly elongated.

Prominent spines appeared around the drop periphery as early as 1 ms after impact, resembling thin blurred lines extending radically in all directions. The drop spread out into a thin liquid film that reached its maximum diameter at approximately 4 ms in all cases. The liquid covered a large portion of the spines as it flowed outwards, so that they became less prominent. Surface tension then pulled liquid backwards, producing a thickening around the rim of the drop. Only partial recoil occurred and some of the blood remained at its maximum extent. The images at 20 ms after impact show drops at rest. The spines were small, but clearly visible around the circumference of the stains. Stain diameter and the magnitude and number of spines increased with initial drop diameter (see Fig. 3 at 20 ms).

Figure 4 shows photographic sequences of blood drop impact on paper in which impact velocity was varied (2.4 m/s, 3.5 m/s, 4.9 m/s), while keeping drop diameter (4.4 mm) constant. Impact dynamics were similar to those seen previously in Fig. 3. The length of spines increased with impact velocity (see Fig. 4 at 2 ms). Raising impact velocity increased stain diameter and also the size and number of spines around stains (Fig. 4 at 20 ms).

Spines around the edges of stains in Figs. 3 and 4 were not evenly distributed, and showed variation in size. Local variations in surface roughness of the paper were responsible for introducing some randomness in the size of spines and also led to some merging of spines. The edge of a 4.3 mm diameter drop landing with 4.2 m/s velocity on paper is magnified in Fig. 5. A Sobel edge detection algorithm (16) was applied to each image in the time series to highlight spines. Spines were clearly leading the spreading liquid film

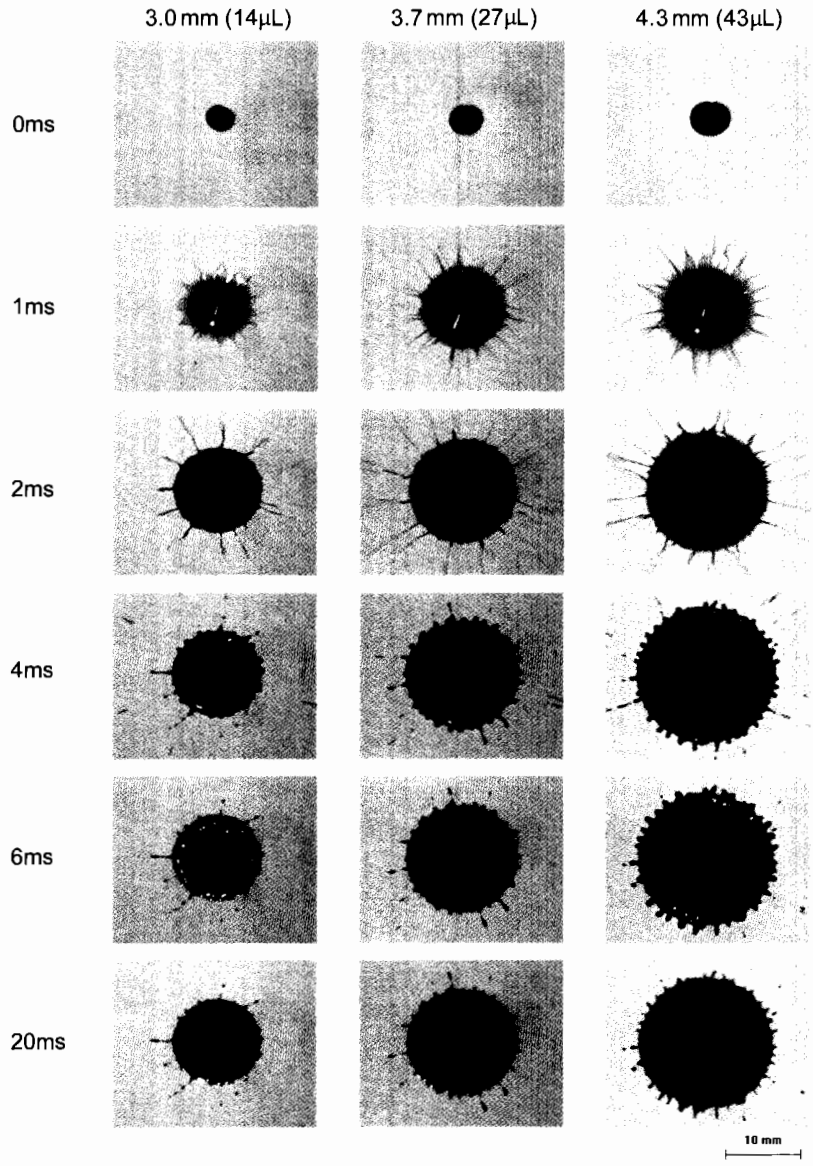

FIG. 3—*A high-speed photograph time series comparing the impact dynamics of three different droplet diameters. Impact velocity was 4.2 m/s and the surface was paper.*

at 1ms. They did not all point in a radial direction, for some were deflected at various angles depending on the resistance encountered while spreading. This led to merging of spines that touched each other, which has been highlighted with an arrow beginning at 1 ms, producing some variation in distribution of spines around stains.

Reducing surface roughness minimizes merging of spines and produces more regular spacing between them. Figure 6 shows photographs of drop impact on three different surfaces with varying average roughness (R_a). They were: glass ($R_a = 0.03$ μm), steel ($R_a = 0.89$ μm) and plastic laminate ($R_a = 1.38$ μm). All were significantly smoother than paper, which had $R_a = 2.92$ μm. The photographs show that the spines were much more symmetrical on these smoother surface and the size of the spines was also much smaller than on paper. Surface roughness promotes fluid instabilities that create spines, amplifying their size. Spines around the final stain on glass, the smoothest surface tested, were so small that they could not be distinguished. (see Fig. 6 at 20 ms). Spines on the other surfaces were small, but clearly visible.

Calculated average values of stain diameter (D_s) are shown in Fig. 7 as a function of initial drop diameter. Stains were photographed from above after the blood had come to rest and drying had commenced. There was no measurable change in stain diameter or number of spines after this time as the blood dried completely. The mean stain diameter was measured using Image Pro Plus analysis software (Media Cybernetics, Silver Spring, MD), taking advantage of the high contrast between the stain and surface. A pixel intensity threshold was first applied to the stain area and the mean diameter was found by taking measurements at 2° intervals passing through the center. Spine length was excluded from this measurement. Each point in Fig. 7 represents the average diameter of 5 stains and error bars their standard deviation. All test surfaces showed an increase in stain diameter with drop diameter. Stain size increased as surface roughness was reduced, so that the largest stains were on glass and the smallest on paper. Stains on steel and plastic, which had similar roughness, were almost identical in diameter.

Figure 8 shows the variation of stain diameter with drop impact velocity (V_o). It confirms the trend seen previously that stain

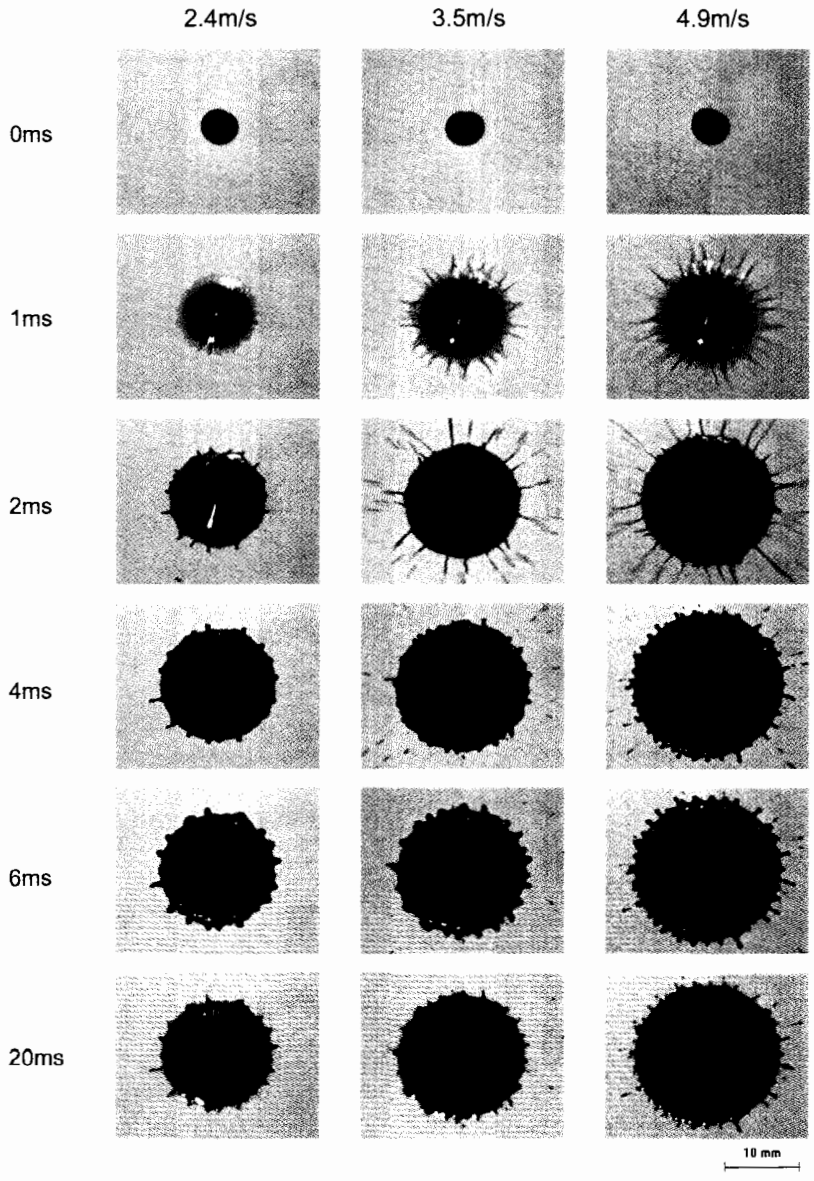

FIG. 4—*A high-speed photograph time series comparing the impact dynamics of three different impact velocities. Droplet diameter was 4.4 mm and the surface was paper.*

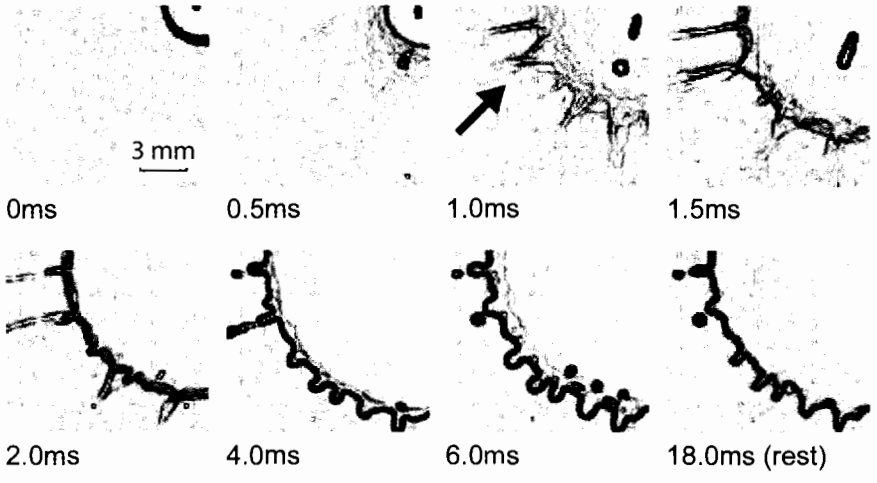

FIG. 5—*Time series of a single droplet impact onto paper. Droplet diameter was 4.3 mm and impact velocity was 4.2 m/s. A Sobel edge detection algorithm was used on the digital images to highlight finger merging. The arrow marks the beginning of two fingers merging.*

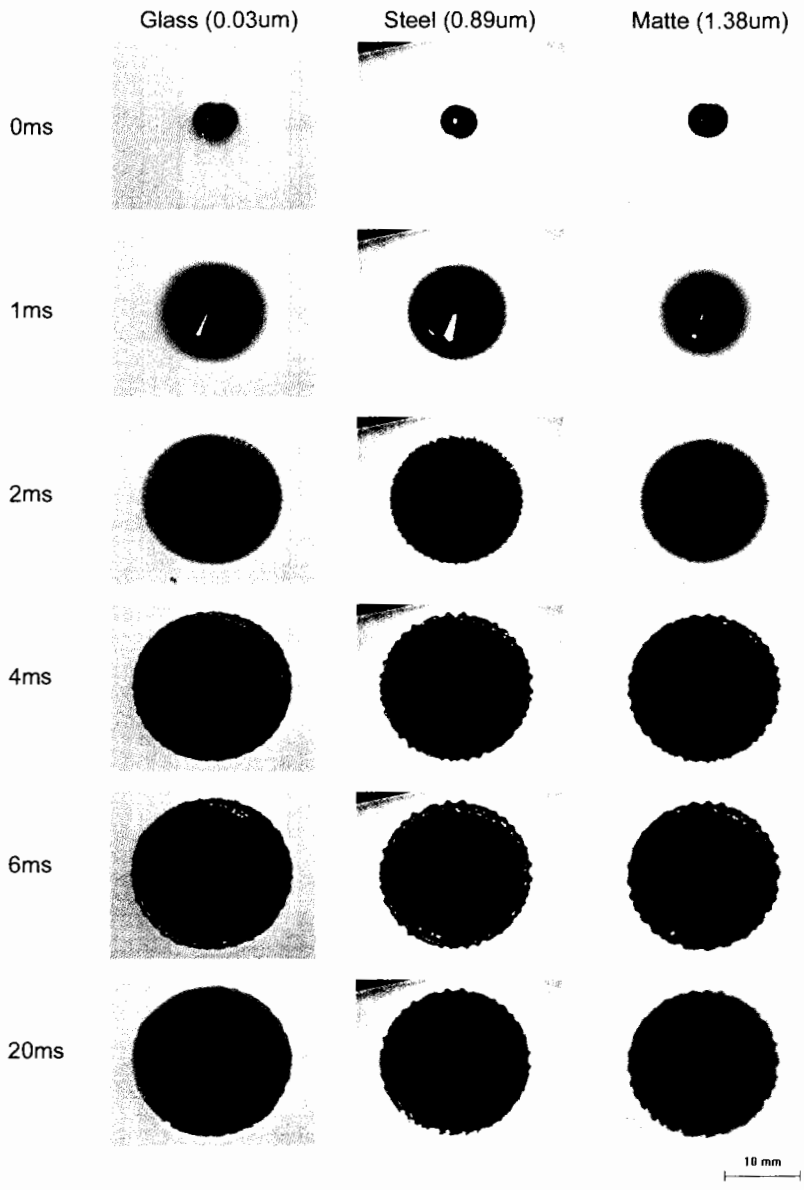

FIG. 6—*A high-speed photograph time series comparing the impact dynamics of three different surfaces. Each surface is shown with the corresponding roughness. A comparable time series for paper is found in Fig. 3. Impact velocity was 4.2 m/s and droplet diameter was 4.3 mm.*

diameter increases with velocity. The largest stains are on glass, the smallest on paper, and there is little difference between those on steel and plastic.

The effect of impact velocity and drop diameter on the number of spines is shown in Figs. 9 and 10 for different surfaces. The spine counting methodology was somewhat subjective. Spines were first defined as any rise and fall above an otherwise smooth outer rim. This included waves, triangles, lines or other protrusions. Spines were counted manually through a complete 360 degrees using the same images acquired to measure stain diameter. While spines were visible for impact on glass at 4 ms, none were observed after the stain had come to rest. Consequently results for glass were omitted from Figs. 9 and 10. Both figures show that the number of spines increases with drop diameter and velocity on all surfaces. However, given the scatter in the data it was difficult to clearly discern a relationship between surface roughness and the number of spines.

Rein (5) has reviewed the extensive literature on drop impact and described analytical models developed to predict maximum drop diameter following impact. When a drop hits a surface the liquid is driven outwards by its inertia, whose magnitude is a function of drop diameter (D_o), impact velocity (V_o) and liquid density (ρ). Drop spread is restrained by viscosity (μ) and surface tension (σ). A drop reaches its maximum spread when these opposing forces balance each other. The ratio of fluid inertia to viscous forces is given by a dimensionless ratio, the Reynolds number (Re) defined as:

$$Re = \frac{\rho D_o V_o}{\mu} \tag{2}$$

Similarly the ratio of inertia to surface tension forces is given by the Weber number (We):

$$We = \frac{\rho D_o V_o^2}{\sigma} \tag{3}$$

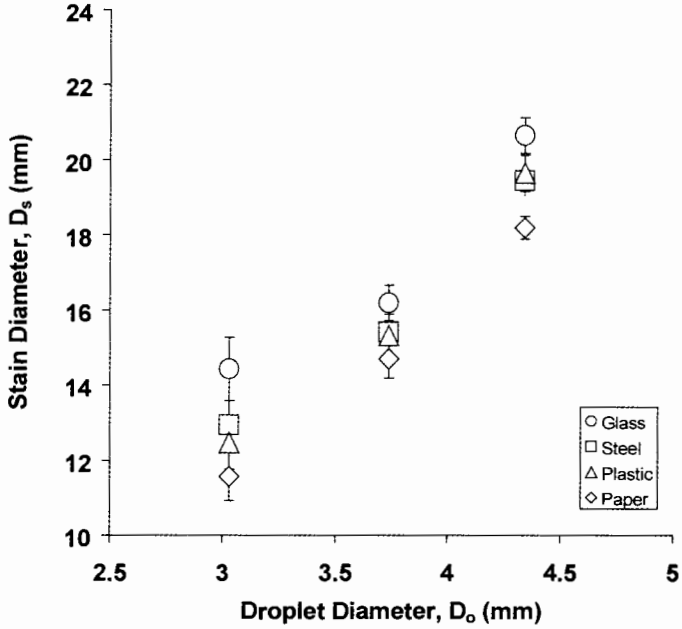

FIG. 7—*The effect of droplet diameter on stain diameter for four surfaces. Impact velocity was 4.2 m/s.*

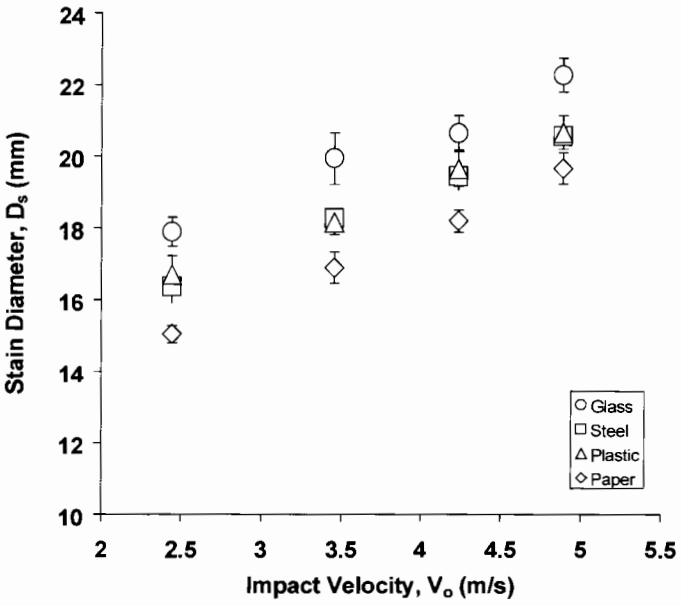

FIG. 8—*The effect of impact velocity on stain diameter for four surfaces. Droplet diameter was 4.3 mm.*

Pasandideh-Fard et al. (6) developed a model to predict maximum drop spread diameter (D_{max}) following impact. They showed that when drop impact inertia was sufficiently high surface tension forces were negligible and maximum drop diameter was a function of Reynolds number alone. This model was tested over a wide range of Reynolds and Weber numbers and found to correlate well with experimental data. Surface tension effects were shown to be negligible if $We \gg Re^{1/2}$, a condition satisfied in our experiments, in which case the maximum spread factor (D_{max}/D_o) was:

$$\frac{D_{max}}{D_o} = \frac{Re^{\frac{1}{4}}}{2} \quad (4)$$

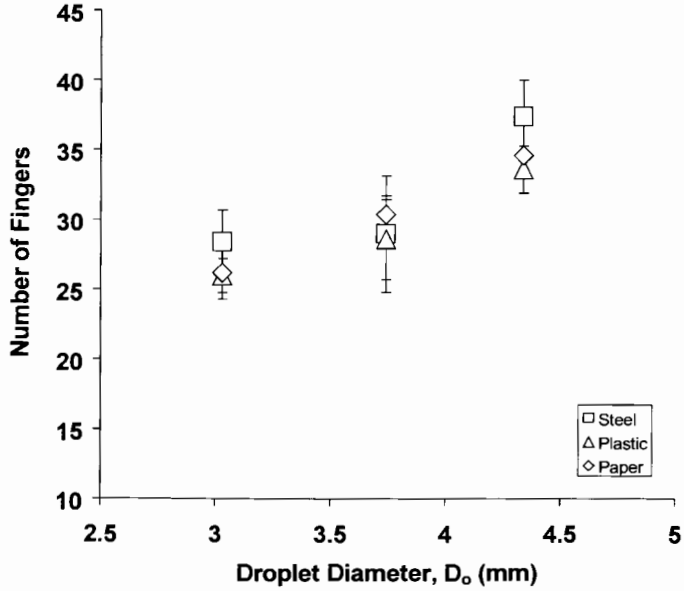

FIG. 9—*The effect of droplet diameter on number of fingers for three surfaces. Impact velocity was 4.2 m/s.*

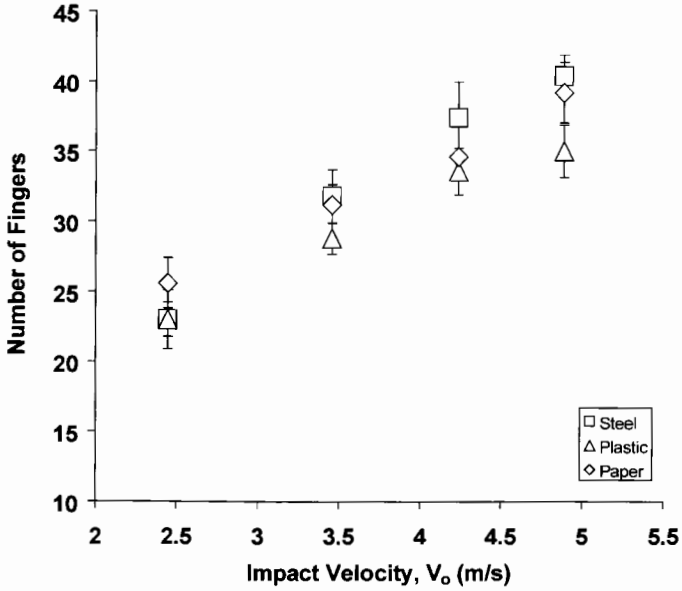

FIG. 10—*The effect of impact velocity on number of fingers for three surfaces. Droplet diameter was kept constant at 4.3 mm.*

Eq 4 predicts D_{max}, the maximum extent of drop spread, not the final stain diameter D_s. However, given that there is little recoil of the drop (see Figs. 3, 4 and 6) we assumed that D_{max} approximately equals D_s. We plotted (see Fig. 11) spread factors, measured from photographs of bloodstains at rest such as those in Figs. 1, as a function of impact Reynolds number, calculated with $\rho = 1062\,kg/m^3$ and $\mu = 0.0048\,kg/ms$. A line representing Eq 4 is also drawn; predictions are seen to lie a little below measured values. The discrepancy may be due to differences between our assumed and actual property values.

Allen (7) suggested that spines form along the edges of spreading drops due to Rayleigh-Taylor instability, which arises when the interface between a liquid and gas is rapidly decelerated, as happens along the rim of a spreading drop. The instability creates undulations on the liquid surface that grow larger and form spines.

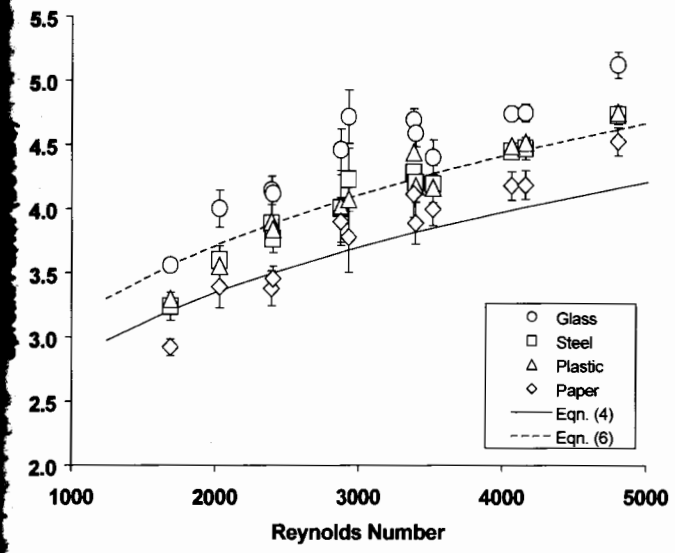

FIG. 11—*Spread factor is plotted against Reynolds number, representing 12 different impact conditions over four surfaces. A model that predicts spread factor is also plotted with and without a correction factor, taken from Eqs 6 and 4, respectively.*

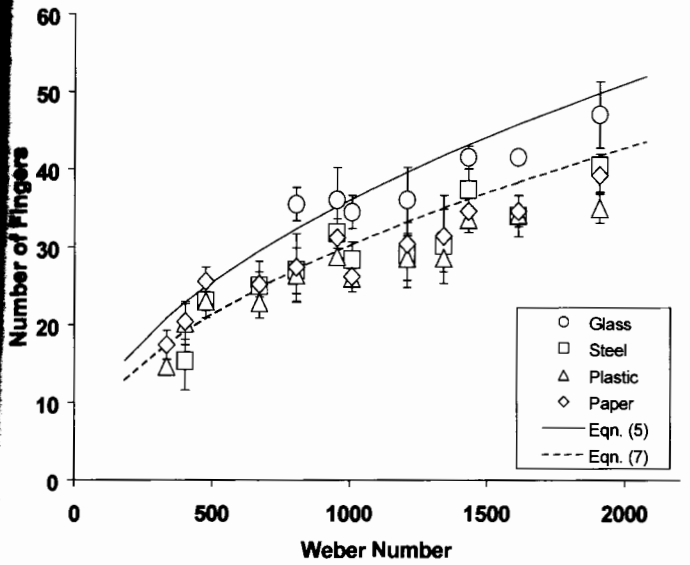

FIG. 12—*Number of fingers is plotted against Weber number, representing 12 different impact conditions over four surfaces. A model that predicts the number of fingers is also plotted with and without a correction factor, taken from Eqs 7 and 5, respectively.*

Thoroddsen and Sakakibara (17) photographed impacting water drops and showed that the number of spines remained constant during drop spread. Kim et al. (8) did a detailed instability analysis and solved the governing equations numerically to calculate the number of spines (N) that would be created for a given set of impact conditions. Mehdizadeh et al. (9) found an analytical solution for the equations and showed that the number of spines could be predicted reasonably accurately by:

$$N = 1.14\sqrt{We} \tag{5}$$

Figure 12 shows the number of spines measured in our experiments around pig bloodstains on four different surfaces. Spines were counted once the drop was at rest, except on the glass surface where spines could not be discerned in the final stain (see Fig. 6); in that case data was taken from photographs at 4 ms. Predictions from Eq 5, calculated with $\sigma = 0.056$ N/m, agree well with the number of spines on glass (Fig. 12). There were fewer spines on the other surfaces, possibly because surface roughness promoted merging of spines.

There is some difference between predictions from Eqs 4 and 5 and experimental measurements, due to uncertainties in property measurements and substrate roughness. To improve agreement between calculated and measured values we introduced two empirical correction factors, C_d and C_n, such that:

$$\frac{D_s}{D_o} = C_d \frac{Re^{\frac{1}{4}}}{2} \tag{6}$$

$$N = 1.14 C_n \sqrt{We} \tag{7}$$

Selecting $C_n = 0.838$ and $C_d = 1.11$ gave the best fits of equations (6) and (7) through experimental data (see Figs. 11 and 12). Using these values we obtained explicit expressions for impact velocity (V_o) and initial drop diameter (D_o) in terms of the number of spines and stain diameter by combining Eqs (6) and (7) with the definitions of Re and We from Eqs (2) and (3):

$$V_o = 0.81 \left(\frac{\sigma^5 N^{10}}{\mu(\rho D_s)^4} \right)^{\frac{1}{9}} \tag{8}$$

$$D_o = 1.67 \left(\frac{D_s^4 \mu}{N\sqrt{\rho\sigma}} \right)^{\frac{2}{9}} \tag{9}$$

Finally, substituting $\rho = 1062$ kg/m^3, $\mu = 0.0048$ kg/ms and $\sigma = 0.056$ N/m, we obtained:

$$V_o = 1.34 \times 10^{-2} \left(\frac{N^5}{D_s^2} \right)^{\frac{2}{9}} \tag{10}$$

$$D_o = 0.324 \left(\frac{D_s^4}{N} \right)^{\frac{2}{9}} \tag{11}$$

Equations 10 and 11 were used to calculate initial drop diameters and impact velocities in our experiments from measurements of bloodstain diameter and number of spines. Fig. 13 compares

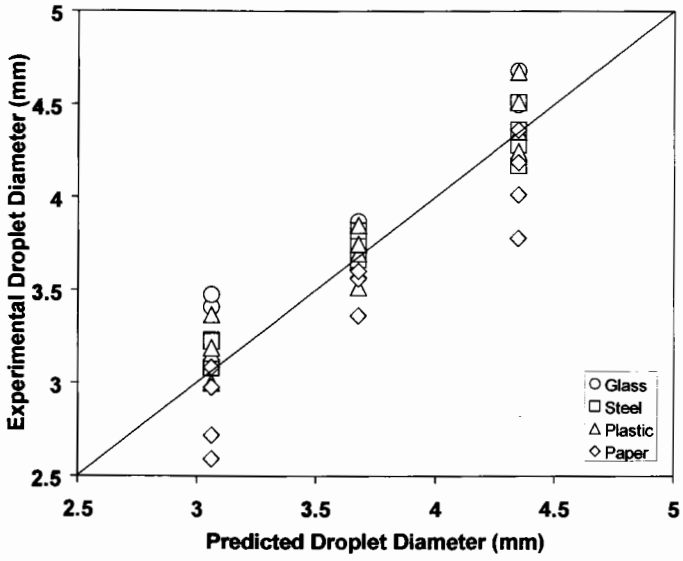

FIG. 13—*Predicted droplet diameter as given by Eq 11 is correlated with experimental droplet diameter.*

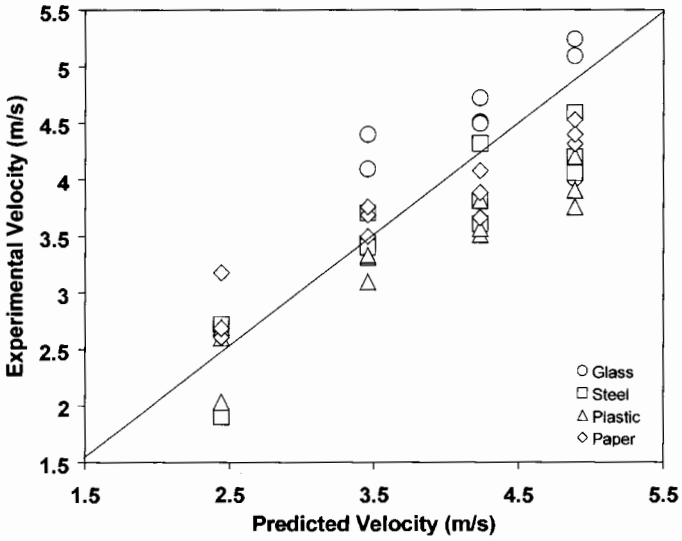

FIG. 14—*Predicted impact velocity as given by Eq 10 is correlated with experimental impact velocity.*

predicted and measured drop diameters, and Fig. 14 impact velocities. The scatter in predicted values is largely due to variations in properties of the four surfaces tested. Surface roughness in our tests varied over two orders of magnitude, from 0.03 μm (glass) to 2.92 μm (paper). For this range of surfaces Eqs 10 and 11 predict droplet diameters within 5% and velocities within 11% on average.

If bloodstains are found at a crime scene on surfaces similar to the ones tested above investigators can measure D_s and N from stains and substitute them in Eqs 10 and 11 to estimate drop diameter and impact velocity. To improve accuracy and provide higher evidentiary value tests should be done for each particular surface on which bloodstains are observed. With this in mind, a simple methodology is proposed for determining droplet velocity and size of a bloodstain found at a crime scene. Investigators should measure D_s and N after properly documenting and photographing the unknown bloodstain. Back at the laboratory, blood drops of known size should be released onto an identical surface from different heights to form stains. Where possible, using a sample of the crime scene surface in question will give the highest accuracy. The spread factor (diameter of stain divided by diameter of droplet) and number of spines should be plotted as a function of *Re* and *We* (defined in Eqs 2 and 3) respectively. Fitting Eqs 6 and 7 through the experimental data—as done in Figs. 11 and 12—will give values for C_n and C_d for the surface being tested. If more precise values of blood properties are available, combining them with the new constants in Eqs 10 and 11 will also improve the precision of drop velocity and size calculations.

Summary and Conclusions

The size of bloodstains and the number of spines around the stain periphery depends on drop impact velocity and drop diameter. It is possible, therefore, to deduce drop size and velocity by measuring stain diameter and counting spines. Errors are introduced into calculations by uncertainties in the physical properties of blood and variations in surfaces on which stains form. We measured the size of pig bloodstains and counted the number of spines formed for different impact conditions. High-speed photographs were taken of impacting drops over a range of impact velocity (2.4–4.9 m/s), drop diameter (3.0–4.3 mm) on four surfaces (glass, steel, plastic, paper) with varying roughness (0.03–2.9 μm). The maximum stain diameter and number of spines increased with impact velocity and drop diameter. Increasing surface roughness reduced stain diameter and promoted merging of spines, diminishing their number. Analytical models were used to obtain simple equations explicitly relating drop diameter and impact velocity to measurements of stain diameter and number of spines. Errors in predicted values were largely due to variations in surface properties. The accuracy of calculations could be improved for a particular surface by observing the size of bloodstains and number of spines on that surface.

The method proposed here could be used in the future by crime scene investigators to estimate blood droplet impact velocity and diameter by substituting them into the appropriate equations. However additional experiments must be conducted before applying this method in casework. Blind studies should be done involving additional substrates and a broader range of blood droplet sizes, as well as a limited number of experiments with human blood (with and without anti-coagulant). In addition the bloodstain criteria imposed for this experiment could be expanded to investigate the effects of non-horizontal surfaces where elliptical droplet patterns are formed. Perhaps a relationship between parent and secondary spatter could be exploited in a similar fashion.

Acknowledgments

We would like to thank the Advanced Optical Microscopy Facility (AOMF) at Princess Margaret Hospital for the use of equipment and image processing software. We would also like to thank Dr. Richard Cobbold for his valuable advice regarding experiments with blood. Funding for this project and to purchase the high-speed camera was provided by grants from the Natural Sciences and Engineering Research Council of Canada.

References

1. MacDonell HL, Bialousz LF. Flight characteristics and stain patterns of human blood. Washington, DC: National Institute of Law Enforcement and Criminal Justice, US Dept of Justice, Law Enforcement Assistance Administration, 1971.
2. Pizzola PA, Roth S, De Forest PR. Blood droplet dynamics—I. J Forensic Sci 1986;31(1):36–49.
3. Laber TL. Blood classification. IABPA News 1985;2(4).
4. Balthazard V, Piedelievre R, Desoille H, DeRobert L. Study of projected drops of blood. Ann Med Leg Criminol Police Sci Toxicol 1939;19: 265–323.
5. Rein M. Phenomena of liquid drop impact on solid and liquid surfaces. Fluid Dyn Res 1993;12:61–93.
6. Pasandideh-Fard M, Bhola R, Chandra S, Mostaghimi J. Capillary effects during droplet impact o a solid surface. Phys Fluids 1996;8:650–9.
7. Allen RF. The role of surface tension in splashing. J Colloid Interface Sci 1975;51(2):350–1.
8. Kim HY, Feng ZC, Chun JH. Instability of a liquid jet emerging from a droplet upon collision with a solid surface. Phys Fluids 2000;12:531–41.
9. Mehdizadeh NZ, Chandra S, Mostaghimi J. Formation of fingers around the edges of a drop hitting a metal plate with high velocity. J Fluid Mechanics 2004;510:353–73.
10. Wonder AY. Blood dynamics. San Diego: Academic Press, 2001.
11. Casson S, Kurland G. Viscometry of human blood for shear rates of 0-100,000 s^{-1}. Nature 1965;206:617–8.
12. Raymond MA, Smith ER, Liesegang J. The physical properties of blood—forensic considerations. Sci Justice 1996;36(3):153–60.
13. Laurent A, Durussek JJ, Dafaux J, Penhouet L, Bailly AL, Bonneau M, et al. Effect of contrast media on blood rheology: comparison in human, pig, and sheep. Cardiovasc Intervent Radiol 1999;22:62–6.

14. Wickham JJ, Bauersachs RM, Wenby RB, Sowernino-Coker S, Meiselman HJ, Elsner R. Red cell aggregation and viscoelasticity of blood from seal, swine and man. Biorheology 1990;27:191–204.
15. Willis C, Piranian AK, Donaggio JR, Barnett RJ, Rowe WF. Errors in the estimation of the distance of fall and angles of impact blood drops. Forensic Sci Int 2001;123(1):1–4.
16. Gonzalez RC, Woods RE. Digital image processing. Reading: Addison Wesley, 1992.
17. Thoroddsen ST, Sakakibara J. Evolution of the fingering pattern of an impacting drop. Phys Fluids 1998;10:1359–74.

Additional information and reprint requests:
Sanjeev Chandra
Department of Mechanical and Industrial Engineering
5 King's College Road
University of Toronto
Toronto, Ontario, Canada, M5S 3G8
E-mail: chandra@mie.utoronto.ca